

See discussions, stats, and author profiles for this publication at: <https://www.researchgate.net/publication/266325844>

The Effect of the Methanol Molecule on the Stabilization of C₁₈H₁₈O₄ Crystal: Combined Theoretical and Structural Investigation.

ARTICLE in THE JOURNAL OF PHYSICAL CHEMISTRY A · SEPTEMBER 2014

Impact Factor: 2.69 · DOI: 10.1021/jp504288r · Source: PubMed

READS

77

10 AUTHORS, INCLUDING:



Ademir J Camargo

Universidade Estadual de Goiás

32 PUBLICATIONS 362 CITATIONS

[SEE PROFILE](#)



Javier Ellena

University of São Paulo

405 PUBLICATIONS 2,656 CITATIONS

[SEE PROFILE](#)



Heibbe Cristhian B. De Oliveira

University of Brasília

41 PUBLICATIONS 346 CITATIONS

[SEE PROFILE](#)



Valter Henrique Carvalho

Universidade Estadual de Goiás, Anápolis, Brazil

14 PUBLICATIONS 40 CITATIONS

[SEE PROFILE](#)

Effect of the Methanol Molecule on the Stabilization of $C_{18}H_{18}O_4$ Crystal: Combined Theoretical and Structural Investigation

Lóide O. Sallum,[†] Hamilton B. Napolitano,[†] Paulo de Sousa Carvalho, Jr.,^{†,||} Amanda Feitosa Cidade,[†] Gilberto Lucio Benedito de Aquino,[†] Nayara D. Coutinho,^{†,§} Ademir J. Camargo,[†] Javier Ellena,^{||} Heibbe C. B. de Oliveira,^{*,§} and Valter H. C. Silva^{*,†,‡}

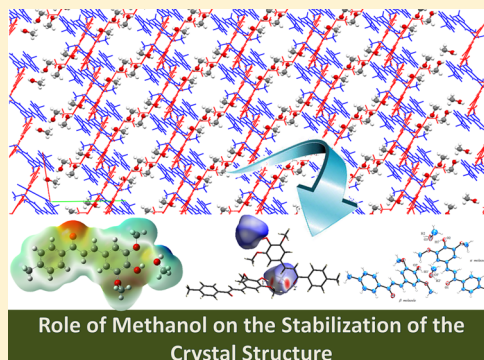
[†]Grupo de Química Teórica e Estrutural de Anápolis, Ciências Exatas e Tecnológicas, Universidade Estadual de Goiás, CP 459, 75001-970 Anápolis, GO Brazil

[‡]Faculdade de Tecnologia SENAI Roberto Mange, 75113-630 Anápolis, GO, Brazil

[§]Laboratório de Modelagem de Sistemas Complexos, Instituto de Química, Universidade de Brasília, Caixa Postal 4478, 70904-970 Brasília, Brazil

^{||}Instituto de Física de São Carlos, Universidade de São Paulo, CP 369, 13560-970 São Carlos, SP, Brazil

ABSTRACT: The ability of the chalcone, $C_{18}H_{18}O_4$, to form solvates was theoretically and experimentally investigated. The unit cell with $Z' > 1$, composed of two independent chalcone molecules (α and β), shows the formation of a stable molecular complex which is related with the presence of methanol in this crystal lattice. Aiming to understand the process of crystal lattice stabilization, a combination of techniques was used, including X-ray diffraction (XRD), computational molecular modeling, and an ab initio molecular dynamic. The results show that α and β molecules are sterically barred from forming a direct hydrogen bond with one other. In addition, the presence of the methanol molecule stabilizes the crystal structure by a bifurcated O—H···O interaction acting as a bridge between them. The theoretical thermodynamic parameter and the rigid potential energy surface scan describe the role of methanol in the energy stabilization of the crystal. The absence of the methanol compound in the asymmetric unit destabilizes the crystalline structure, making the formation process of the asymmetric unit nonspontaneous. The energy difference between α and β molecules is around 0.80 kcal·mol⁻¹, indicating that both are stable and equally possible in the crystal lattice. The analysis of the energy profile of the C14—O2···H1—O3 and O2—H1···O3—C17 torsion angles in the crystal packing shows that the α and β molecules are confined in the stable potential region, in agreement with the two conformers in the asymmetric unit. The Molecular Electrostatic Potential (MEP) shows that the methanol has no steric effects, which prevents small motion around the torsion angles.



1. INTRODUCTION

The molecular arrangement in the crystal lattice determines the fundamental properties of the material, such as stability, solubility, color, strength,^{1,2} and as a result, its pharmacological/technological applications. In this regard, the crystallization of organic compounds is the crucial step in lattice formation, and the solvent molecule is a fundamental variable associated with the process. The solvent may have significant effects, providing conditions for the formation of different types of packages, as well as its inclusion in the lattice composition.^{3–6} Many substances with specific features can form solvates under vapor pressures. Inclusion of the solvent in the crystal lattice requires a molecular recognition process in which stable hydrogen bonds and interaction motifs are generated, leading to a stabilization of the crystal lattice and the formation of the solvates.^{7,8}

Solvate substances are multicomponent crystals with the solvent molecule hosted in the crystal lattice; they can be stoichiometric or nonstoichiometric.^{6,9} In both solvate types,

the guest molecule is an essential part of the structure because it affects not only the thermodynamic and kinetic properties but also the mechanical properties associated with crystal packing.^{10,11} In a previous paper, Xue and co-workers¹² showed that changing the crystallization process of benzohydrazide derivatives leads to the formation of monohydrated and unsolvated solid forms. This property was associated with the existence of short hydrogen bonds and the incorporation of solvent molecules that optimize the cohesion of the molecular arrangement. Additionally, the examination of the solvent's molecular recognition preferences has guided the design of new solvates. Recently, Aitipamula¹⁰ synthesized six new sulfamerazine solvates, considering the hydrogen bonded networks mediated by the solvent molecules. Particularly, some studies^{13–15} have shown that methanol, acetone, benzene,

Received: May 1, 2014

Revised: September 29, 2014



dichloromethane, and toluene are the most frequent guest solvents when only organic structures are analyzed. These molecules are able to form multiple and stable hydrogen bond motifs with the organic solute molecule.

Chalcones consist of open-chain flavonoids which can be obtained by Claisen–Schmidt condensation between aromatics ketones and aldehyde^{16,17} and constitute an important group of natural and synthetic products. Considering the crystal lattice of chalcones and elucidated derivatives, there are few examples of bundling with the inclusion of a solvent in the crystal lattice.¹⁸ Chalcones have received much attention due to their relatively simple synthesis process, simple structure, and the variety of pharmacological activities reported for them. The class is reported to have anti-inflammatory, antimalarial, antiviral, antibacterial, antifungal, and antitumor activities.^{16,17,19–22}

Based on our interest in the chemistry of chalcones^{23,24} and their applications, our research group has synthesized and elucidated the chalcone (*E*)-3-(4-hydroxy-3,5-dimethoxyphenyl)-1-*p*-tolylprop-2-en-1-one (Figure 1) and noted a non-

bath. Then, 9 mL of a solution of NaOH (50% w/v) was added, followed by 0.41g (2.24 mmol) of syringaldehyde. The resulting solution was stirred at room temperature for 24 h, and after this time, the medium reaction was poured into iced water and neutralized with a 50% HCl solution. The resulting precipitate was filtered, washed with water, and purified by recrystallization from methanol. The solid obtained showed yellow coloration: mp 85.2–87.6 °C. ¹H NMR (500 MHz) (CDCl₃): 2.46 (s, 3 H, CH₃Ph); 3.86 (s, 6 H, OCH₃Ph); 6.55 (t, 1H, PhCH, *J* = 2.44 Hz); 6.80 (d, 2H, PhCH, *J* = 2.44 Hz); 7.33 (d, 2 H, PhOCH₃, *J* = 8.54 Hz); 7.50 (d, 1H, CHCO, *J* = 15.56 Hz); 7.73 (d, 1H, CHPh, *J* = 15.56 Hz); 7.95 (d, 2H, PhOCH₃, *J* = 8.24 Hz). IR (KBr) cm^{−1}: 3240(O–H); 3050, 2940; 1680 (C=O); 1320.

2.3. Crystallization and Crystallographic Characterization. The compound C₁₈H₁₈O₄ was crystallized from methanol in 5 days by the slow evaporation technique. The X-ray diffraction data for title compound were collected at room temperature using a KAPPA-CCD Diffratometer with graphite-monochromated Mo K α radiation (λ = 0.71073 Å). The structure was solved by Direct Methods and anisotropically refined with full-matrix least-squares on F² using SHELXL97.²⁸ The hydrogen atoms were placed at calculated positions and refined with riding constraints. The cell refinements were performed using the software Collect²⁹ and Scalepack.³⁰ Data reduction was carried out using the software Denzo-SMN and Scalepack.³⁰ Molecular representation, tables, and pictures were generated by WinGX,³¹ ORTEP-3,³² and MERCURY 2.2³³ programs. The Hirshfeld surfaces^{34,35} and the associated 2D fingerprint plots were calculated using Crystal Explorer.³⁶ The structure was deposited at the Cambridge Crystallographic Data Center under the number CCDC 984420. Copies of the data can be obtained, free of charge, via www.ccdc.cam.ac.uk.

2.4. Computational Details. The geometrical and atomic numbering used in the calculations for asymmetric units are shown in Figure 1. The electronic structure of single-molecule calculations of the asymmetric unit was investigated within Kohn–Sham Density Functional Theory (DFT).^{37,38} Starting from X-ray structure, we carried out a single-point calculation with 6-31g(d) Pople's split-valence basis set and used the exchange–correlation functional of Perdew and co-workers as modified by Adamo and Barone (mPWPW91).³⁹ We explored this exchange–correlation functional because it has been successfully used in prediction on the thermodynamically properties.⁴⁰ The interaction energy (ΔE) between two chalcones interacting with a specific methanol was calculated in the presence and absence of the solvent (methanol).

Although we know that the removal of the solvent can lead to a completely different molecular packing, we assume in our calculations that the removal of methanol does not alter the molecular arrangement. The interaction energy was calculated based on the interaction process: α molecule + β molecule \rightarrow 2[(C₁₈H₁₈O₄)·(CH₃OH)] (see nomenclature in Figure 2a). The interaction energies included a basis set superposition error (BSSE) due to the supermolecule approach using the full counterpoise method developed by Boys and Bernardi.^{41–43} The zero-point vibrational energy (ZPVE) contributions were non-negligible in the calculation of interaction energy. Furthermore, the Gibbs free energy was calculated for the interaction process. The partial atomic charges employed in this work were the charges derived from the map of electrostatic potential (ESP), using the Merz–Singh–Kollman (MSK) scheme.^{44,45} In this scheme, the partial atomic charges are

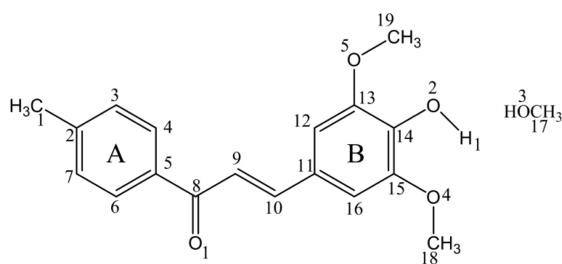


Figure 1. Composition of the asymmetric unit, Z' > 1. Structural formula of compound C₁₈H₁₈O₄ and methanol.

conventional fact: a unit cell with multiple components (Z' > 1) generating a complex molecular packing resulted from the existence of methanol in the crystal lattice. Each chalcone molecule exhibits its own supramolecular packing which is connected by the methanol molecules. Multiple molecules in the asymmetric unit have considerable interest and, in general, can be rationalized in terms of the special requirements for the formation of hydrogen bonds in crystals.^{25–27}

In the present paper, we introduce the crystal structure of C₁₈H₁₈O₄, and a detailed analysis of its crystal packing and conformational features are presented comparatively using computational methods. In addition, we performed a comprehensive study of the molecular recognition between this chalcone and the methanol solvent.

2. EXPERIMENTAL PROCEDURE

2.1. General. Organic reagents were purchased from Aldrich or Fisher and were used without further purification. Melting points (mp) were determined using a Mel-Temp instrument and are uncorrected. Infrared (IR) spectra were recorded using a PerkinElmer Frontier FT-IR instrument as films on KBr discs, unless otherwise stated. ¹H NMR spectra were obtained using a Varian Unity Inova 500 instrument unless otherwise stated. Chemical shifts are reported in parts per million (ppm) downfield from internal tetramethylsilane (Me₄Si). The reaction progress was assessed by thin-layer chromatography (TLC) using Merck silica gel (60 F254) on aluminum plates unless otherwise stated.

2.2. Synthesis. 4-Methylacetophenone (0.3003 g, 2.24 mmol) was added to a 25 mL flask and was cooled in an ice

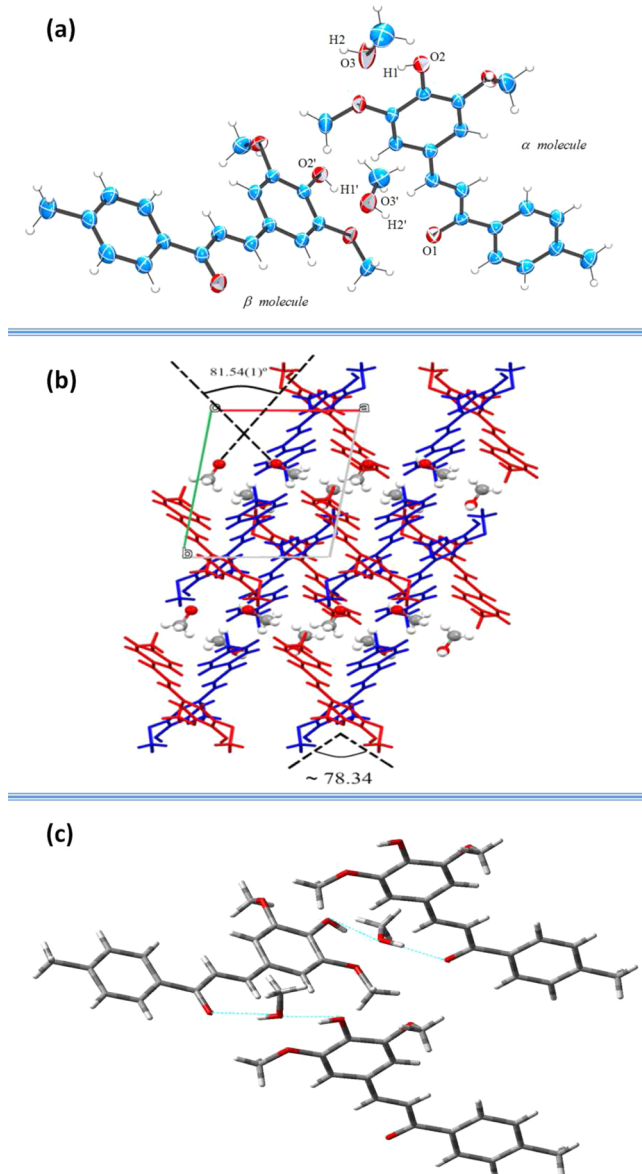


Figure 2. (a) Displacement ellipsoids are shown at the 30% probability level, and atomic numbering follows Figure 1. The chalcones interacting with a specific methanol receive the nomenclature: α molecule and β molecule. (b) A view of molecule packing showing hydrogen bond for α molecule (in red) and β molecule (in blue). (c) Schematic interpretation of networks associated with α and β molecules in the crystal structure of $C_{18}H_{18}O_4$.

fitted to the electrostatic potential at points selected according to the MSK scheme, with the same level of calculation.

The rigid potential energy surface scan was performed over a rectangular grid involving the selected $C14-O2-H1\cdots O3$ and $O2-H1\cdots O3-C17$ torsion angles (see Figure 1) at mPWPW91/6-31g(d) level of calculations, considering the molecular environment of an approximately parallelepiped shape. The selected torsion angles of the α molecule were stepped 35 times by increasing by 10 degrees each time. In the rigid scan, ZPVE contributions were negligible. Molecular dynamic trajectories of 20 000 steps with a time step of 0.100 fs were calculated using the Atom centered Density Matrix Propagation (ADMP) molecular dynamic,^{46,47} with an initial kinetic energy of 100 mH (milli-Hartree). Unit cells of compounds were replicated along the [001] direction,

generating a supercell of an approximately parallelepiped shape. The molecular dynamic of the parallelepiped block was optimized using the semiempirical method PM6,⁴⁸ and this level of calculation was chosen considering a large molecular system. All theoretical calculations were carried out using the Gaussian 09 program suite.⁴⁹

3. RESULTS AND DISCUSSION

3.1. Crystal Structure of Compound $C_{18}H_{18}O_4$. The (*E*)-3-(4-hydroxy-3,5-dimethoxyphenyl)-1-*p*-tolylprop-2-en-1-one crystallizes in the triclinic centrosymmetric $P\bar{1}$ space group as a solvate structure. The asymmetric unit is described by a 2-[($C_{18}H_{18}O_4$)·(CH_3OH)] molecular complex, in which each independent $C_{18}H_{18}O_4$ molecule is bonded to a specific methanol molecule. Both α molecule and β molecules exhibit statically similar correspondent bond lengths, angles, and torsion angles. The compound consists of two substituted aromatic rings (A and B) connected by a propanone chain. The torsion angle between two aromatic rings is 8.90° for α molecule and 6.49° for β molecule. The molecular conformation is almost planar (rms deviation of the non-H atoms from the mean plane formed by the chalcone skeleton is 0.001 Å), except for the largest deviation of $O5-C19$ group (-1.066 and 1.055 Å for α and β molecules, respectively). The A ring shows a methyl group at *para* position while B ring bearers $O-CH_3$ groups substituent are at *para* and *ortho* position and a -OH group [- $O2'-H1'$] attached to C14'. The $C9'-C10'$ bond length of 1.324(3) Å for α molecule and $C9-C10$ bond length of 1.328(3) Å for β molecule are indicative of significant double-bond character. Detailed crystal structure data are summarized in Table 1.

Table 1. Crystal Data and Structure Refinement of $C_{18}H_{18}O_4$

formula weight	330.38	
temperature (K)	293(2)	
color	yellow	
cell dimensions (Å)	$a = 8.651(1)$ Å	$\alpha = 105.587(4)$ °
	$b = 12.015(2)$ Å	$\beta = 90.972(5)$ °
	$c = 17.786(2)$ Å	$\gamma = 97.498(5)$ °
volume (Å ³)	1762.9(3)	
Z, Z'	4, 2	
F(000)	704	
crystal size (mm)	0.29 × 0.14 × 0.11	
θ range for data acquisition	2.91° to 26.37°	
refine reflections/parameters	7108/445	
solve/refinement method	direct method/least-squares full matrix	
goodness-of-fit on F^2	1.007	
R factor [$I > 2\sigma(I)$]	$R_1 = 0.0636, wR_2 = 0.1595$	
R factor (all data)	$R_1 = 0.1237, wR_2 = 0.1869$	

The overall low crystal symmetry corroborates the existence of 2-[($C_{18}H_{18}O_4$)·(CH_3OH)] complex in the asymmetric unit. In the molecular complex, α and β molecules show different spatial orientation in which molecules are twisted by the 78.34° that is consistent with the observed values for the orientation of α and β solvent, see Figure 2b. The $C_{18}H_{18}O_4$ molecule has a hydroxyl group that is positioned between bulky groups which provide electronic repulsion (methoxyl groups) and make a direct interaction between the α and β molecules of donor and acceptor groups difficult. Considering the polarity and the small size of methanol molecules, their presence as an entity stabilizes the crystal structure through a bifurcated hydrogen bond

[O2'–H1'…O3'; O3'–H2'…O1'; O2–H1…O3; O3–H2…O1']. Indeed, the arrangement enables the connection between α and β molecules by a C18–H18…C_{gB} (Table 2) resulting from the electron distribution difference in A and B ring.

Table 2. Hydrogen-Bond Geometry (Distances (Å) and Angles (deg))^a

D–H…A	D–H	D…A	H…A	D–H…A
O2–H1…O3 ⁽⁰⁾	0.820	2.633(2)	1.864	155.70
O2'–H1'…O3' ⁽⁰⁾	0.820	2.668(2)	1.893	157.10
O3'–H2'…O1 ⁽⁰⁾	0.820	2.784(2)	1.981	166.03
C10–H10…O4 ⁽⁰⁾	0.930	3.639(2)	2.748	160.73
C9–H9…O5 ⁽¹⁾	0.931	3.394(2)	2.648	137.54
C4–H4A…O5 ⁽¹⁾	0.930	3.574(2)	2.718	153.50
C19–H19F…O1 ⁽²⁾	0.960	3.677(2)	2.765	159.07
C4'–H4'…O5 ⁽³⁾	0.930	3.605(2)	2.776	148.96
C12'–H12'…O5 ⁽³⁾	0.929	3.508(2)	2.739	140.67
C10'–H10'…O4 ⁽⁴⁾	0.931	3.651(2)	2.790	154.27
C19'–H19C…O1 ⁽⁵⁾	0.960	3.726(2)	2.797	162.94
C1'–H1D…O3 ⁽⁵⁾	0.960	3.733(2)	2.844	154.36
C17'–H17B…O1 ⁽⁶⁾	0.960	3.615(2)	2.770	147.25
O3–H3…O1 ⁽⁷⁾	0.820	2.753(2)	1.936	173.93
C18–H18F…C _{gB} ^b	0.960	3.637(2)	3.605	119.62

^aThe numbers in the parentheses reflect uncertainty in the last digit in each measurement. Symmetry code: (0) x, y, z (1) $-x, -y, -z + 1$ (2) $-x + 1, -y, -z + 1$ (3) $-x + 1, -y, -z + 2$ (4) $x + 1, +y, +z$ (5) $-x + 2, -y, -z + 2$ (6) $-x + 1, -y - 1, -z + 1$ (7) $x - 1, +y, +z$. ^bC_{gB}: centroid formed by C11' → C16'

Despite the conformational similarity, each independent molecule has its own hydrogen-bonded network. The α and β molecules are involved in three hydrogen bonds of type O–H…O and two hydrogen bonds of type C–H…O (Table 2). The intermolecular O2'–H1'…O3' hydrogen bond involving the C17'–O3' methanol molecule and O2'–H1' hydroxyl moieties with the intermolecular O3'–H2'…O1 hydrogen bond involving the C17'–O3' methanol molecule and C8=O1 carbonyl connect the two molecules which are shown in Figure 2(c). The O2–H1…O3 is an intermolecular interaction between the *non* prime chalcone molecule with its own solvent, which presents an O2…O3 distance and O2–H1…O3 angle 2.633(3) Å and 155.70(2) $^\circ$, respectively, resulting in the alignment of the hydroxyl group and the methanol molecule. Similarly, the O2'–H1'…O3' intermolecular contact orients the O2'–H1' group of prime molecules to the O3' oxygen atom of β solvent. Concerning the crystal packing, the 2-[C₁₈H₁₈O₄](CH₃OH)] molecular complex is stabilized in three ways: (1) the first involves the O3–H2…O1' hydrogen bond which propagates it along [100] direction; (2) in the second one, the β -methanol promotes the formation of a 2D-network by O3'–H2'…O1 and C17–H17B…O1 linking adjacent molecular complexes along [100] direction; (3) finally, C17'–H17B…O1 generates a hydrogen-bond three-dimensional network, which is shown in Table 2.

The Hirshfeld surface and its fingerprint plots are complementary tools for systematic description of the same molecule in different crystal environments. The Hirshfeld surface is a measurement of the space occupied by a given molecule in the crystal and summarizes information from all interactions and molecular contacts simultaneously.³⁵ The two-dimensional fingerprint plots are derived from the Hirshfeld surface, which provides a summary of the frequency of each

combination of d_e (i.e., the distance from the surface to the nearest atom in the molecule itself) and d_i (i.e., distance from the surface to the nearest atom in another molecule) across the surface of a molecule. Two-dimensional fingerprint plots were generated by using the d_i and d_e pairs measured at each individual spot of the calculated Hirshfeld surface. This information shows not only the set of present interactions but also the relative area of the surface corresponding to each such interaction. Blue color corresponds to the low frequency of occurrence of (d_e, d_i) pair, while red points indicate the high frequency of the surface points with that (d_e, d_i) combination.

Figure 3 shows the Hirshfeld surface and its fingerprint plots of α and β molecules. In the fingerprint plots, the prominent sharp spike denoted by 1 and 2 refer to dominant O–H…O interactions between methanol and carboxyl group of chalcones. The denomination (') in the indices 1 and 2 distinguish the two solvent molecules. As the fingerprint plots are decomposed by interactions, some differences are evidenced for α and β molecule solvents: (i) The selective highlighting of the C…H intermolecular contacts shows an effective difference between the molecular environments of α and β molecules; (ii) The two-dimensional fingerprint of solvent molecules results in a proportion of intermolecular contacts H…O/O…H and H…C/C…H in the area of the surface which contribute 25.9% and 11.3% for α solvent and 28.5% and 2.7% for β solvent, respectively. These differences in the molecular environment are less obvious when analyzing the packing diagram. These results corroborate the fact that there is different spatial orientation for each solvent in the crystal of the title compound that is reflected directly in the supramolecular lattice, with different packing for α and β molecules.

3.2. Energies and Molecular Geometries. The crystallographic analyses of the chalcone lattice crystal provide a consistent suggestion about the role of methanol in the stabilization of the crystal and the difference in the arrangement of its packing. A theoretical analysis of this chalcone can offer a complete understanding of the stabilization and packing of the crystal from energy and geometric parameters.

The role of methanol in the stabilization of the crystal can be described by energy and thermodynamic properties. The thermodynamic properties, interaction energy (ΔE) and Gibbs free energy (ΔG), for α and β molecules in the asymmetric unit with and without the methanol molecule, are presented in Table 3. As expected, the zero-point vibrational energy (ZPVE) correction is similar for both conformers with and without the methanol molecule. As shown, the energy difference between α and β molecules is very small (about 0.8 kcal·mol⁻¹). The interaction energy between α and β molecules is -84.27 kcal·mol⁻¹, showing a strong stabilization of the asymmetric unit due to the presence of the methanol compound. Additionally, the value of Gibbs free energy is presented, -65.12 kcal·mol⁻¹, and it is possible to observe that the formation of the asymmetric unit is highly spontaneous. The thermodynamic parameters for the stabilization of the asymmetric unit, without methanol, are also presented with interaction energy of -2.29 kcal·mol⁻¹ and Gibbs free energy of 11.53 kcal·mol⁻¹. This fact shows that the absence of the methanol compound destabilizes the crystalline structure, making the stabilization process of the asymmetric unit nonspontaneous.

The role of methanol in the energy stabilization of the structure was determined considering only crystallographic analysis and is in agreement with theoretical thermodynamic

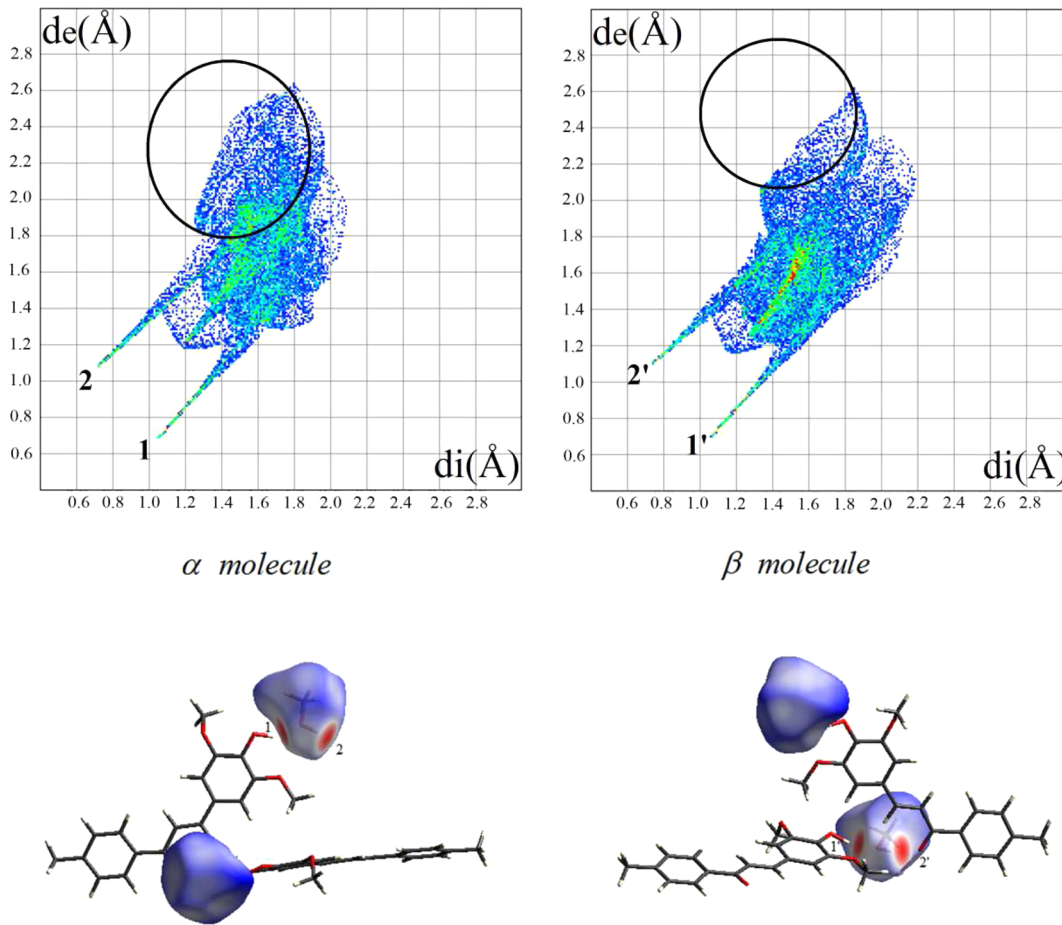


Figure 3. Hirshfeld surface and two-dimensional fingerprint plots for α and β molecules. Color scale for surface between -0.693 au (blue) to 1.550 au (red). The fingerprint plots also evidence the different packing modes of the two solvent molecules. The Hirshfeld surface shows a significant difference in the proportion of $\text{C}\cdots\text{H}/\text{H}\cdots\text{C}$ contacts (in black circles).

Table 3. Total Energies, Zero-Point Vibration Energy (ZPVE), Interaction Energy (ΔE), and Gibbs Free Energy (ΔG) Calculated for α and β Molecules with BSSE Correction^a

	with methanol			without methanol		
	α molecule	β molecule	asymmetric unit	α molecule	β molecule	asymmetric unit
energy	-1112.6030	-1112.6017	-2225.2182	-996.8852	-996.99025	-1993.9836
ZPVE	0.3989	0.3991	0.6773	0.3381	0.3380	0.6773
ΔG correction	0.3541	0.3539	0.6178	0.2974	0.2972	0.6178
ΔE (BSSE)		-84.27			-2.29	
ΔG (BSSE)		-65.12			11.53	

^aThe asymmetric unit is built with and without methanol and calculated at mPWPPW91/6-31g(d) level of calculation. Energy, ZPVE and correction to Gibbs energy are in Hartree. ΔE and ΔG are in $\text{kcal}\cdot\text{mol}^{-1}$.

properties. Additionally, this behavior can be connected with theoretical geometric parameters and contributes to the understanding of the packing in the supramolecular arrangement. Table 4 presents the calculated and experimental geometric parameters, which show a significant difference. The large divergence between calculated and experimental structure is around the carboxyl group and the solvent (methanol) group, because the crystal packing is not considered in the calculated structure, allowing significant modifications close to donor and acceptor groups. The other geometric parameters in the α and β molecules are very similar. As pointed out in the crystallography analysis, the main difference between the α and β molecules are $\text{C}14-\text{O}2-\text{H}1-\text{O}3$ and $\text{O}2-\text{H}1-\text{O}3-\text{C}17$ torsion angles. Figure 4a shows the

overlap between both X-ray structures, with a focus on the differences in these torsion angles. The α and β molecules calculated have similar geometric parameters. This result was expected, because in the optimization process, the crystal environment for α and β molecules is not considered. The values for $\text{C}14-\text{O}2\cdots\text{H}1-\text{O}3$ and $\text{O}2-\text{H}1\cdots\text{O}3-\text{C}17$ torsion angles are -99.85° and -5.07° , respectively. In addition, there are significant differences for the geometric parameter around carboxyl and methanol groups (for example $\text{C}8-\text{C}9-\text{C}10$, $\text{C}14-\text{O}2-\text{H}1$, $\text{O}2-\text{H}1-\text{O}3$, and $\text{H}1-\text{O}3-\text{C}17$ angles) between X-ray and optimized structure. These results reflect the deep influence of the structure packing in the stabilization of the methanol and chalcone.

Table 4. Calculated (mPW91/6-31g(d) and PM6) and Experimental Geometric Parameters (Distances (\AA) and Angles (deg)) for α and β Molecules

	α molecule (mPW91/6-31g(d))	β molecule (mPW91/6-31g(d))	α molecule (X-ray)	β molecule (X-ray)	α molecule (PM6)
bonds					
C ₁ –C ₂	1.49(8)	1.49(8)	1.51(0)	1.50(4)	1.49(3)
C ₂ –C ₃	1.38(8)	1.38(8)	1.38(3)	1.39(3)	1.40(5)
C ₃ –C ₄	1.38(5)	1.38(5)	1.38(0)	1.37(7)	1.39(6)
C ₄ –C ₅	1.39(0)	1.39(0)	1.38(8)	1.38(5)	1.40(2)
C ₅ –C ₆	1.39(4)	1.39(4)	1.38(6)	1.38(8)	1.40(5)
C ₆ –C ₇	1.37(8)	1.37(8)	1.37(7)	1.37(8)	1.39(3)
C ₇ –C ₂	1.39(4)	1.39(4)	1.37(9)	1.36(8)	1.40(6)
C ₅ –C ₈	1.48(9)	1.48(9)	1.48(7)	1.48(4)	1.49(3)
C ₈ –O ₁	1.21(6)	1.21(6)	1.23(0)	1.23(9)	1.21(8)
C ₈ –C ₉	1.47(2)	1.47(2)	1.46(2)	1.46(0)	1.48(7)
C ₉ –C ₁₀	1.33(8)	1.33(8)	1.32(8)	1.32(4)	1.34(0)
C ₁₁ –C ₁₂	1.45(1)	1.45(1)	1.45(3)	1.45(5)	1.47(3)
C ₁₂ –C ₁₃	1.39(3)	1.39(3)	1.39(6)	1.40(1)	1.40(9)
C ₁₃ –C ₁₄	1.37(9)	1.37(9)	1.37(7)	1.37(2)	1.41(3)
C ₁₄ –C ₁₅	1.40(0)	1.40(0)	1.38(3)	1.39(1)	1.41(6)
C ₁₅ –C ₁₆	1.40(0)	1.40(0)	1.40(5)	1.40(4)	1.39(3)
C ₁₆ –C ₁₁	1.38(1)	1.38(1)	1.37(4)	1.38(4)	1.40(8)
C ₁₄ –O ₂	1.39(5)	1.39(5)	1.40(0)	1.39(0)	1.36(7)
O ₂ –H ₁	0.97(8)	0.97(8)	0.82(0)	0.82(0)	1.04(0)
H ₁ –O ₁₇	1.75(0)	1.75(1)	1.86(4)	1.89(3)	1.72(2)
angles					
C ₅ –C ₈ –C ₉	119.1(1)	119.1(1)	119.4(0)	119.5(1)	117.2(6)
C ₅ –C ₈ –O ₁	119.7(0)	119.7(0)	119.7(6)	119.3(9)	121.0(5)
C ₈ –C ₉ –C ₁₀	119.4(0)	119.4(0)	123.9(5)	123.8(8)	120.8(5)
C ₉ –C ₁₀ –C ₁₁	128.0(2)	128.0(2)	127.6(3)	127.6(1)	124.1(0)
C ₁₄ –O ₂ –H ₁	113.4(8)	113.4(8)	109.4(9)	109.4(8)	111.1(4)
O ₂ –H ₁ –O ₃	163.5(8)	163.5(0)	155.7(0)	157.1(0)	146.0(4)
H ₁ –O ₃ –C ₁₇	109.7(3)	109.7(0)	116.5(3)	116.6(2)	107.4(5)
torsion angles					
C ₅ –C ₈ –C ₉ –C ₁₀	176.4(3)	176.4(4)	-178.2(9)	-177.1(4)	167.1(2)
C ₈ –C ₉ –C ₁₀ –C ₁₁	179.3(4)	179.3(4)	179.7(5)	-179.7(6)	-179.8(2)
C ₁₄ –O ₂ –H ₁ –O ₃	-99.8(6)	-99.9(8)	167.9(0)	-178.2(1)	-99.5(6)
O ₂ –H ₁ –O ₃ –C ₁₇	-5.0(8)	-5.0(7)	-18.3(7)	2.3(9)	-33.9(7)

To evaluate the sensitivity of the C₁₄–O₂···H₁–O₃ and O₂–H₁···O₃–C₁₇ torsion angles in the crystal packing, we measured the potential energy surface (PES) for these torsion angles (Figure 4b). We can observe that the α and β molecules are confined in the stable potential region (dark blue), indicating that the α and β molecules, in the crystal structure, are equally probable, showing that both possibilities can be observed in the asymmetric unit. Additionally, Figure 4b shows the existence of a large region of minimum energy and enables the existence of the other stable conformations of methanol in the crystal around C₁₄–O₂···H₁–O₃ and O₂–H₁···O₃–C₁₇ torsion angles. However, the intermolecular contact CH₃OH···O=C limits the existence of the other conformations, stabilizing the crystal with only two possibilities per asymmetric unit. These results indicate that the methanol molecule occupies a minimum region supposed to be a molecular cavity^{25,27} which assists in the packing of the methanol and consequently in the stabilization of the crystal structure. A real view of the molecular cavity can be seen from the molecular dynamic simulation, as presented in subsection 3.4.

3.3. Molecular Electrostatic Potential (MEP). The MEP is associated with electronic density and is an important property to explain sites of reactivity as well as their interactions.⁴¹ Electric charges in the molecule are the driving

force for electrostatic interactions.^{41,50,51} Thus, the MEP is also a useful property to provide the specific information about the processes of the interaction of one molecule with another. The MEPs for the α molecule with and without methanol are represented in Figure 5a,b, respectively. The negative MEP corresponds to the region of high electron density; it is seen in the proximity of the oxygen atoms, in red color, specifically in the carbonyl and hydroxyl groups. The α molecule without methanol shows O₁, O₂, O₄ and O₅ with charged values around -0.521, -0.483, -0.323 and -0.359, respectively. The α molecule with methanol does not undergo significant modifications at charge values in the oxygen atoms and presents a charge for the O₃ (methanol) around -0.652. The value for the charge of O₁ and O₂ shows small discrepancies which should be explained by the interaction patterns for these atoms, which are involved in a hydrogen bond in the crystal structure.

Figure 5a shows that the methanol has no steric effect, which prevents small motion around the torsion angles as presented in Figure 4. In other words, this electrostatic distribution allows slight variations and the existence of the α and β molecules.

3.4. Molecular Dynamics. In order to investigate the temporal evolution of the methanol trapped inside of the crystal structure, an atom centered density matrix propagation

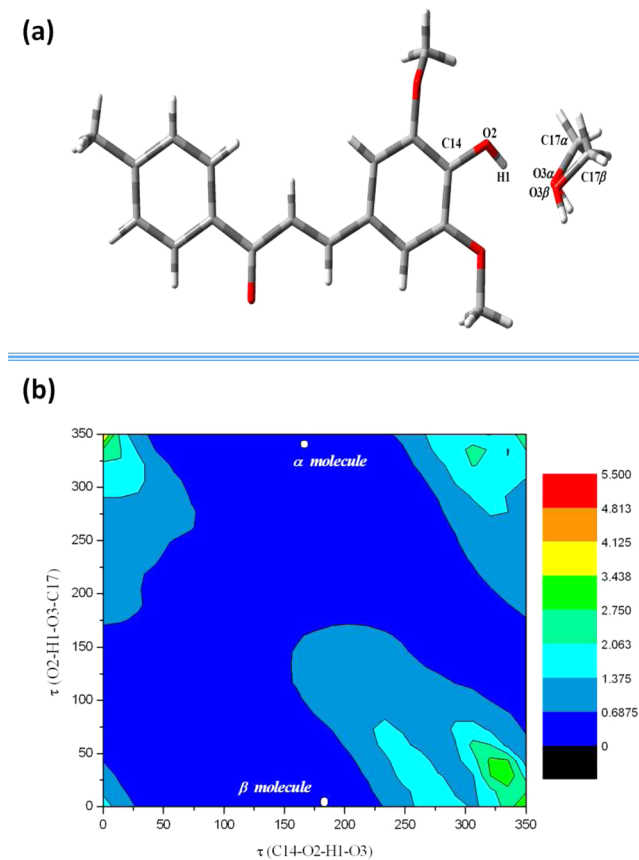


Figure 4. (a) Overlap between α and β molecules. (b) Conformational analysis (rigid scan) around $C14-O2\cdots H1-O3$ and $O2-H1\cdots O3-C17$ torsion angles of (*E*)-3-(3,4,5-trimethoxyphenyl)-1-(4-biphenyl)-prop-2-en-1-one calculated at the mPWPW91/6-31g(d) level of calculation. The unit energy is in $\text{kcal}\cdot\text{mol}^{-1}$.

molecular dynamics model (ADMP) as implemented in Gaussian 09 package was carried out on a system of 368 atoms taken directly from crystallographic structure as discussed previously. As shown in Table 4 the PM6 semiempirical method is able to reproduce the geometric parameters of the compound under study. As this method can be applied to large molecular systems with relatively low computational costs, it was selected for the present simulation. The system was simulated for 2 ps in the NVE ensemble

without any kind of geometric constraint (i.e., all degrees of freedom were allowed to fluctuate during the simulation). The first 1 ps was used in the equilibration phase, and the last picosecond was used for production. The system had been sampling at each 0.100 fs and averaged for analysis.

Molecular dynamic trajectories of the crystal structure present a description of the continuum process under analysis. Figure 6 shows the time-evolution of the torsion angles for unit

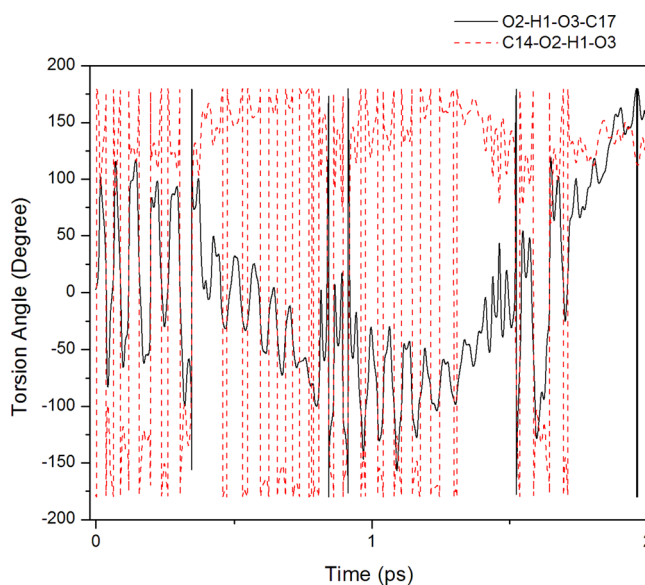


Figure 6. Temporal evolution of the $C14-O2-H1-O3$ and $O2-H1-O3-C17$ torsion angles at PM6 level for the β molecule.

cells of the title compound in the crystal environment. Interestingly, the torsion angles have a periodic behavior, accessing various conformational possibilities around the methanol molecule. The torsion angle $O2-H1-O3-C17$ includes the hydrogen bond $H1-O3$. This bond is the axis that allows the mobility of methanol in crystal structure in a periodic behavior as Figure 6 shows.

Figures 7 is a noticeable formation of α and β molecules in the first steps (Figures 7a,b) and the subsequent steps (Figure 7e,f) of the dynamic, showing that these two conformations are equally probable. In other steps of the dynamic (Figures 7c,d) other conformational possibilities arise (due to the molecular

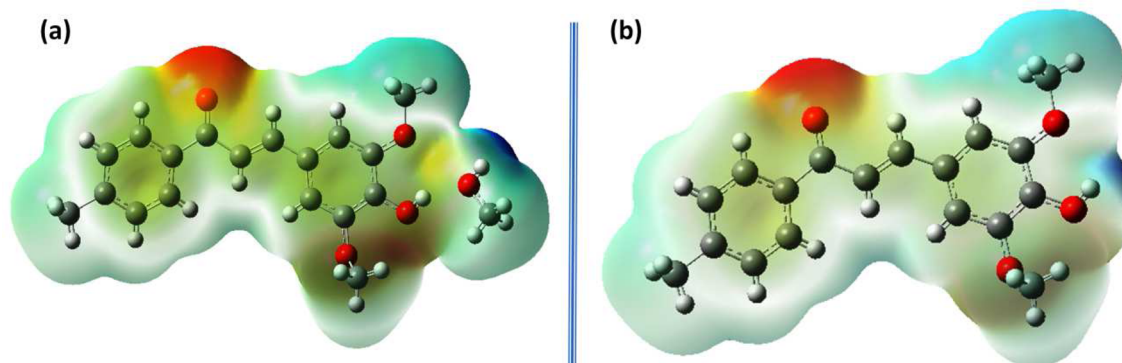


Figure 5. MEP of the α molecule based on MK scheme calculated at mPWPW91/6-31g(d) level of calculation (a) with and (b) without methanol. The red color represents the maximum negative charge value, the blue color represents the maximum positive charge value, and the other colors represent the intermediate charges values.

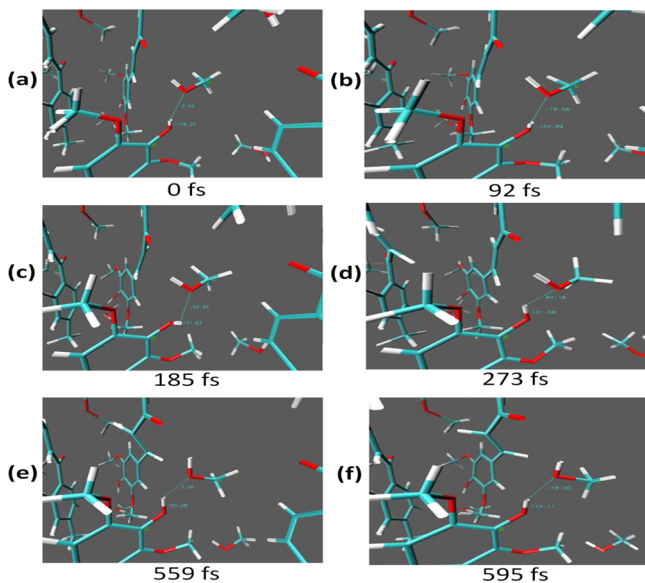


Figure 7. Typical snapshots of molecular structure along a trajectory showing the methanol around chalcone compound.

cavity presented in the rigid scan – Figure 4b), but these are not observed in the crystal system.

4. CONCLUSION

The compound $C_{18}H_{18}O_4$ crystallized in the $P\bar{1}$ space group with two methanol and two chalcone molecules composing the asymmetric unit ($Z' = 2$). The solvent molecules differ in the orientation of torsion angles that correlates them with chalcone molecules. DFT optimized structural parameters are close to those observed in X-ray diffraction. Methanol is a molecular entity that stabilizes the crystal structure through a bifurcated hydrogen bond [$O2'-H1'...O3'$; $O3'-H2'...O1'$; $O2-H1...O3$; $O3-H2...O1'$], forming two independent conformers in the asymmetric unit (α and β molecules). The theoretical thermodynamic parameters show that the absence of the methanol compound in the asymmetric unit could destabilize the crystalline structure, making the stabilization process of the asymmetric unit nonspontaneous. The energy difference between α and β molecules is around $0.80 \text{ kcal}\cdot\text{mol}^{-1}$, indicating that both conformers are stable and are equally possible in the crystal lattice. The analysis of the energy profile of the $C14-O2-H1-O3$ and $O2-H1-O3-C17$ torsion angles in the packing crystal show that the α and β molecules are confined to the stable potential region, in agreement with the two conformers in the asymmetric unit. The MEP shows that the methanol has no steric effect, which prevents small motion around the torsion angles.

■ AUTHOR INFORMATION

Corresponding Authors

*E-mail: fatioleg@gmail.com. Phone: +55 61 3107-3899. Fax: +55 61 3273-4149 (V.H.C. Silva).

*E-mail: heibbe@unb.br. Phone: +55 61 3107-3899. (H.C.B. de Oliveira).

Notes

The authors declare no competing financial interest.

■ ACKNOWLEDGMENTS

The authors would like to acknowledge the following Brazilian agencies for financial support: Conselho Nacional de Desenvolvimento Científico e Tecnológico (CNPq), Coordenação de Aperfeiçoamento de Pessoal de Nível Superior (CAPES), and Fundação de Amparo à Pesquisa do Estado de São Paulo (FAPESP).

■ REFERENCES

- (1) Kerns, E.; Di, L. *Drug-like Properties: Concepts, Structure Design and Methods: From ADME to Toxicity Optimization*; Elsevier Science, London, 2010.
- (2) Basavouj, S.; Boström, D.; Velaga, S. Indomethacin–Saccharin Cocrystal: Design, Synthesis and Preliminary Pharmaceutical Characterization. *Pharm. Res.* **2008**, *25*, 530–541.
- (3) Fox, D. *Physics and Chemistry of the Organic Solid State 1*; Interscience Publishers: New York, 1963.
- (4) Brittain, H. G. *Polymorphism in Pharmaceutical Solids*. Marcel Dekker: New York, 1999.
- (5) Morissette, S. L.; Soukase, S.; Levinson, D.; Cima, M. J.; Almarsson, Ö. Elucidation of Crystal form Diversity of the HIV Protease Inhibitor Ritonavir by High-throughput Crystallization. *Proc. Natl. Acad. Sci. U.S.A.* **2003**, *100*, 2180–2184.
- (6) Hilfiker, R. *Polymorphism: In the Pharmaceutical Industry*; Wiley: Weinheim, 2006.
- (7) Borka, L. Review on Crystal Polymorphism of Substances in the European Pharmacopoeia. *Pharm. Acta. Helv.* **1991**, *66*, 16–22.
- (8) Halebian, J. K. Characterization of Habits and Crystalline Modification of Solids and Their Pharmaceutical Applications. *J. Pharm. Sci.* **1975**, *64*, 1269–1288.
- (9) Aakeroy, C. B.; Forbes, S.; Desper, J. The Effect of Water Molecules in Stabilizing Co-crystals of Active Pharmaceutical Ingredients. *CrystEngComm* **2012**, *14*, 2435–2443.
- (10) Aitipamula, S.; Chow, P. S.; Tan, R. B. H. The Solvates of Sulfamerazine: Structural, Thermochemical, and Desolvation Studies. *CrystEngComm* **2012**, *14*, 691–699.
- (11) Vangala, V. R.; Chow, P. S.; Tan, R. B. H. The Solvates and Salt of Antibiotic Agent, Nitrofurantoin: Structural, Thermochemical and Desolvation Studies. *CrystEngComm* **2013**, *15*, 878–889.
- (12) Xue, L.-W.; Han, Y.-J.; Zhao, G.-Q.; Feng, Y.-X. Synthesis, Characterization and Crystal Structures of N'-(5-Bromo-2-hydroxybenzylidene)-2-fluorobenzohydrazide in Unsolvated and Monohydrate Forms. *J. Chem. Crystallogr.* **2011**, *41*, 1599–1603.
- (13) Gorbitz, C. H.; Hersleth, H.-P. On the Inclusion of Solvent Molecules in the Crystal Structures of Organic Compounds. *Acta Crystallogr., Sect. B: Struct. Sci.* **2000**, *56*, 526–534.
- (14) Stoica, C.; Verwer, P.; Meekes, H.; van Hoof, P. J. C. M.; Kaspersen, F. M.; Vlieg, E. Understanding the Effect of a Solvent on the Crystal Habit. *Cryst. Growth Des.* **2004**, *4*, 765–768.
- (15) Hu, W.-J.; Liu, L.-Q.; Ma, M.-L.; Zhao, X.-L.; Liu, Y. A.; Mi, X.-Q.; Jiang, B.; Wen, K. m-Terphenyl-3,3"-dioxo-derived Oxacalixaromatics: Synthesis, Structure, and Solvent Encapsulation in the Solid State. *Tetrahedron* **2013**, *69*, 3934–3941.
- (16) Rao, Y. K.; Fang, S.-H.; Tzeng, Y.-M. Synthesis and Biological Evaluation of 3',4',5'-trimethoxychalcone Analogues as Inhibitors of Nitric Oxide Production and Tumor Cell Proliferation. *Bioorg. Med. Chem.* **2009**, *17*, 7909–7914.
- (17) Wu, J.; Wang, C.; Cai, Y.; Peng, J.; Liang, D.; Zhao, Y.; Yang, S.; Li, X.; Wu, X.; Liang, G. Synthesis and Crystal Structure of Chalcones as well as on Cytotoxicity and Antibacterial Properties. *Med. Chem. Res.* **2012**, *21*, 444–452.
- (18) Allen, F. The Cambridge Structural Database: A Quarter of a Million Crystal Structures and Rising. *Acta Crystallogr., Sect. B: Struct. Sci.* **2002**, *58*, 380–388.
- (19) Bandgar, B. P.; Gawande, S. S.; Bodade, R. G.; Gawande, N. M.; Khobragade, C. N. Synthesis and Biological Evaluation of a Novel Series of Pyrazole Chalcones as Anti-inflammatory, Antioxidant and Antimicrobial Agents. *Bioorg. Med. Chem.* **2009**, *17*, 8168–8173.

- (20) Vanchinathan, K.; Bhagavannarayana, G.; Muthu, K.; Meenakshisundaram, S. P. Synthesis, Crystal Growth and Characterization of 1,5-diphenylpenta-1,4-dien-3-one: An Organic Crystal. *Physica B* **2011**, *406*, 4195–4199.
- (21) Silva, W. A.; Andrade, C. K. Z.; Napolitano, H. B.; Vencato, I.; Lariucci, C.; Castro, M. R. C. d.; Camargo, A. J. Biological and Structure-activity Evaluation of Chalcone Derivatives Against Bacteria and Fungi. *J. Braz. Chem. Soc.* **2013**, *24*, 133–144.
- (22) Nowakowska, Z. A Review of Anti-infective and Anti-inflammatory Chalcones. *Eur. J. Med. Chem.* **2007**, *42*, 125–137.
- (23) Alvim, H. G. O.; Fagg, E. L.; de Oliveira, A. L.; de Oliveira, H. C. B.; Freitas, S. M.; Xavier, M.-A. E.; Soares, T. A.; Gomes, A. F.; Gozzo, F. C.; Silva, W. A.; et al. Probing Deep into the Interaction of a Fluorescent Chalcone Derivative and Bovine Serum Albumin (BSA): An Experimental and Computational Study. *Org. Biomol. Chem.* **2013**, *11*, 4764–4777.
- (24) Oliveira, G.; Oliveira, H.; Silva, W.; Silva, V.; Sabino, J.; Martins, F. Structure and Theoretical Approaches to a Chalcone Derivative. *Struct. Chem.* **2012**, *23*, 1667–1676.
- (25) Bishop, R.; Scudder, M. L. Multiple Molecules in the Asymmetric Unit ($Z' > 1$) and the Formation of False Conglomerate Crystal Structures[†]. *Cryst. Growth Des.* **2009**, *9*, 2890–2894.
- (26) Stahly, G. P. Diversity in Single- and Multiple-Component Crystals. The Search for and Prevalence of Polymorphs and Cocrystals. *Cryst. Growth Des.* **2007**, *7*, 1007–1026.
- (27) Steed, J. W. Should Solid-state Molecular Packing Have to Obey the Rules of Crystallographic Symmetry? *CrystEngComm* **2003**, *5*, 169–179.
- (28) Sheldrick, G. A Short History of SHELX. *Acta Crystallogr., Sect. A: Found. Crystallogr.* **2008**, *64*, 112–122.
- (29) Hooft, R. W. W. COLLECT; Nonius BV: Delft, The Netherlands, 1998.
- (30) Otwinowski, Z.; Minor, W. *Methods in Enzymology: Macromolecular Crystallography, Part A*; Academic Press: New York, 1997.
- (31) Farrugia, L. WinGX Suite for Small-molecule Single-crystal Crystallography. *J. Appl. Crystallogr.* **1999**, *32*, 837–838.
- (32) Farrugia, L. ORTEP-3 for Windows - A Version of ORTEP-III With a Graphical User Interface (GUI). *J. Appl. Crystallogr.* **1997**, *30*, S65–S65.
- (33) Macrae, C. F.; Edgington, P. R.; McCabe, P.; Pidcock, E.; Shields, G. P.; Taylor, R.; Towler, M.; van de Streek, J. Mercury: Visualization and Analysis of Crystal Structures. *J. Appl. Crystallogr.* **2006**, *39*, 453–457.
- (34) Spackman, M. A.; McKinnon, J. J. Fingerprinting Intermolecular Interactions in Molecular Crystals. *CrystEngComm* **2002**, *4*, 378–392.
- (35) McKinnon, J. J.; Spackman, M. A.; Mitchell, A. S. Novel Tools for Visualizing and Exploring Intermolecular Interactions in Molecular Crystals. *Acta Crystallogr., Sect. B: Struct. Sci.* **2004**, *60*, 627–668.
- (36) Wolff, S. K.; Grimwood, D. J.; McKinnon, J. J.; Jayatilaka, D.; Spackman, M. A. *Crystal Explorer 2.1*; University of Western Australia: Perth, Australia, 2007.
- (37) Hohenberg, P.; Kohn, W. Inhomogeneous Electron Gas. *Phys. Rev.* **1964**, *136*, B864–B871.
- (38) Kohn, W.; Sham, L. J. Self-Consistent Equations Including Exchange and Correlation Effects. *Phys. Rev.* **1965**, *140*, A1133–A1138.
- (39) Adamo, C.; Barone, V. Exchange Functionals With Improved Long-range Behavior and Adiabatic Connection Methods Without Adjustable Parameters: The mPW and mPW1PW Models. *J. Chem. Phys.* **1998**, *108*, 664–675.
- (40) Sousa, S. F.; Fernandes, P. A.; Ramos, M. J. General Performance of Density Functionals. *J. Chem. Phys. A* **2007**, *111*, 10439–10452.
- (41) Breneman, C. M.; Wiberg, K. B. Determining Atom-centered Monopoles From Molecular Electrostatic Potentials. The Need for High Sampling Density in Formamide Conformational Analysis. *J. Comput. Chem.* **1990**, *11*, 361–373.
- (42) Sedano, P. S. *Implementation and Application of Basis Set Superposition Error-correction Schemes to the Theoretical Modeling of Weak Intermolecular Interactions*; University of Girona: Girona, 2001.
- (43) Salvador, P.; Duran, M. The Effect of Counterpoise Correction and Relaxation Energy Term to the Internal Rotation Barriers: Application to the BF₃···NH₃ and C₂H₄···SO₂ Dimers. *J. Chem. Phys.* **1999**, *111*, 4460–4465.
- (44) Singh, U. C.; Kollman, P. A. An Approach to Computing Electrostatic Charges for Molecules. *J. Comput. Chem.* **1984**, *5*, 129–145.
- (45) Besler, B. H.; Merz, K. M.; Kollman, P. A. Atomic Charges Derived From Semiempirical Methods. *J. Comput. Chem.* **1990**, *11*, 431–439.
- (46) Iyengar, S. S.; Schlegel, H. B.; Millam, J. M.; A. Voth, G.; Scuseria, G. E.; Frisch, M. J. Ab initio Molecular Dynamics: Propagating the Density Matrix With Gaussian Orbitals. II. Generalizations Based on Mass-weighting, Idempotency, Energy Conservation and Choice of Initial Conditions. *J. Chem. Phys.* **2001**, *115*, 10291–10302.
- (47) Schlegel, H. B.; Iyengar, S. S.; Li, X.; Millam, J. M.; Voth, G. A.; Scuseria, G. E.; Frisch, M. J. Ab initio Molecular Dynamics: Propagating the Density Matrix With Gaussian Orbitals. III. Comparison with Born–Oppenheimer Dynamics. *J. Chem. Phys.* **2002**, *117*, 8694–8704.
- (48) Stewart, J. P. Optimization of Parameters for Semiempirical Methods V: Modification of NDDO Approximations and Application to 70 Elements. *J. Mol. Model.* **2007**, *13*, 1173–1213.
- (49) Frisch, M. J.; Trucks, G. W.; Schlegel, H. B.; Scuseria, G. E.; Robb, M. A.; Cheeseman, J. R.; Scalmani, G.; Barone, V.; Mennucci, B.; Petersson, G. A.; et al. *Gaussian 09, Rev. A.02*; Gaussian, Inc.: Wallingford CT, 2009.
- (50) Kestner, N. R. He–He Interaction in the SCF–MO Approximation. *J. Chem. Phys.* **1968**, *48*, 252–257.
- (51) Boys, S. F.; Bernardi, F. The Calculation of Small Molecular Interactions by the Differences of Separate Total Energies. Some Procedures With Reduced Errors. *Mol. Phys.* **1970**, *19*, 553–566.